Laser self-induced thermo-optical effects in a magnetic fluid

Shengli Pu,[a] Xianfeng Chen,[b] Weijun Liao, Lijun Chen, Yuping Chen, and Yuxing Xia
Department of Physics, Institute of Optics and Photonics, The State Key Laboratory on Fiber Optic Local Area Communication Networks and Advanced Optical Communication Systems, Shanghai Jiao Tong University, Shanghai 200240, China

(Received 17 May 2004; accepted 27 August 2004)

The laser self-induced thermo-optical effects in a magnetic fluid are studied in this work. We study the origin of these effects theoretically, and then experiments are done to investigate the relationship between the divergence angle of the laser beam and the incident power. From the experimental results, we find out that the divergence angle increases linearly with the incident power to some critical power, which is in good agreement with the theory. To the high incident power side, the divergence angle will deviate from the linear relationship and the spherical aberration interference rings will be blurred due to the occurrence of the convective currents. © *2004 American Institute of Physics*. [DOI: 10.1063/1.1808242]

Magnetic fluid (MF) is a stable colloid consisting of finely divided single-domain magnetic nanoparticles (usually 3–15 nm in diameter) coated with a molecular layer of dispersant and dispersed in a suitable liquid carrier.[1] The MF we usually use today was first synthesized in the early 1960s. For a long period of time, almost all the attentions of researchers are focused on its mechanical and magnetic properties and few on its optical properties.[2,3] Recently, with the dramatic development of optical communication and integrated optics, many researchers' interests are drawn to its optical characteristics under an applied magnetic field (called magneto-optical properties),[4–9] and the potential applications to optical devices based on these properties have been proposed, for example, optical switches,[4] tunable optical gratings.[5]

Although the optical properties of MF have been studied intensively in recent years, most of the work is focused on the optical anisotropy under an external magnetic field. The researches on the optical properties under the influence of heat produced by the laser itself are underway and the reports about these are rare.[10–13] Because thermal effects play an important role in the pragmatic applications of the devices, it is significant to study these effects further. In this paper, we will report the laser self-induced thermo-optical effects in a magnetic fluid and the power-dependent relationship is highlighted.

When a laser beam passes through the MF, it will heat the MF and create a temperature gradient in it, and meanwhile, its concentration will be redistributed. These two factors will cause the change of refractive index and make the MF act like a lens, which is called the thermal lens effect.[14–16] It has been confirmed to be a very effective method for measuring the small absorption coefficients of liquids and solids.[17–19] Recently, Marcano *et al.* have reported that they have measured absorption coefficients as small as 10^{-8} cm^{-1} by this effect.[19] While MF has a large optical absorption coefficient, the influence of the thermal lens effect is focused on the divergence of the laser beam after passing through it and the spherical aberration interference rings in the far field.

Considering a Gaussian beam of fundamental mode, the temperature distribution in the MF can be expressed as[14]

$$\Delta T(r,t) = \frac{A w_0^2}{8\kappa}\left(Ei\left(-\frac{2r^2}{w_0^2}\right) - Ei\left(-\frac{2r^2}{8Dt + w_0^2}\right)\right), \quad (1)$$

where $A = 0.48\ \alpha P/\pi/w_0^2$, $D = \kappa/\rho/C$, $t_c = w_0^2/4/D$, and r is the transverse distance from the laser beam-centered optical axis (centimeter), w_0 is the spot radius of the laser beam on the MF (centimeter), κ, D, ρ, C, and α are the thermal conductivity, the thermal diffusivity, the mass density, the specific heat, and the absorption coefficient of the MF, respectively. Their units are $cal\ cm^{-1}\ s^{-1}\ k^{-1}$, $cm^2\ s^{-1}$, $g\ cm^{-3}$, $cal\ g^{-1}\ k^{-1}$, and cm^{-1}, respectively. P is the total incident power (watts), t_c is the characteristic time for the thermal conduction (s), and Ei is the exponential integral.

Because of the large absorption of MF, Eq. (1) should be multiplied by $e^{-\alpha z}$ (z is the direction of the beam propagation). So, the temperature gradient at (r,z,t) in the MF for the steady state ($t \gg t_c$ or $t \cdot D \gg 1$) is expressed by

$$\frac{\partial[(\Delta T(r,z)]}{\partial r} = \frac{A w_0^2}{4\kappa}\frac{1}{r}(e^{-2r^2/w_0^2} - 1)e^{-\alpha z}. \quad (2)$$

We define the divergence angle θ as the included angle between the beam rays and the centered axis of the laser beam, which can be expressed by[20]

$$\theta(r,z) = \left|\frac{\partial}{\partial r}\int_0^L \frac{\delta n(r,z)}{n_0} dz\right|, \quad (3)$$

[a]Electronic mail: shlpu@sjtu.edu.cn
[b]Electronic mail: xfchen@sjtu.edu.cn

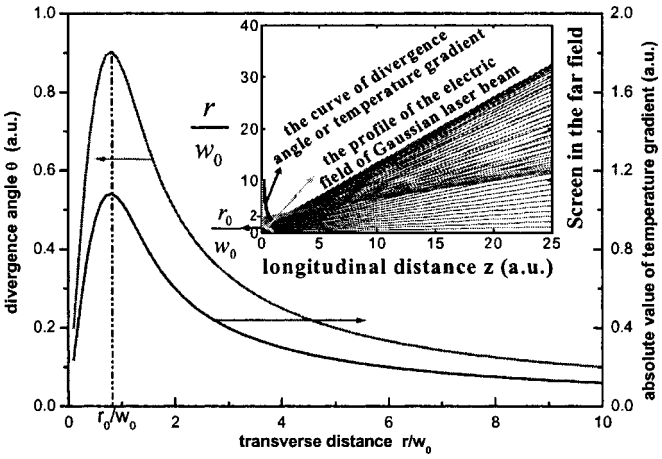

FIG. 1. (Color online) Divergence angle θ and the absolute value of the temperature gradient $|\partial(\Delta T(r,z))/\partial r|$ as a function of r/w_0. The inset shows the propagation of the beam rays in the free space after passing through the MF.

where L and n_0 are the thickness and the refractive index of the MF. The change of refractive index induced by the thermal expansion and concentration redistribution is given as[21]

$$\frac{dn(r,z)}{dT} = \left.\frac{\partial n}{\partial T}\right|_c + \frac{\partial n}{\partial c}\frac{\partial c}{\partial T}, \tag{4}$$

where $(\partial n/\partial T)|_c$ and c are the thermo-optical coefficient and the concentration of the MF and T is the temperature.

With Eqs. (2) and (3), and $A=0.48\ \alpha P/\pi/{w_0}^2$, the divergence angle can be derived to be

$$\theta(r) = \frac{0.12\ P}{\pi\kappa n_0}\left|\frac{dn}{dT}\right|(1-e^{-\alpha L})\frac{1-e^{-2r^2/{w_0}^2}}{r}. \tag{5}$$

Figure 1 plots the divergence angle versus r/w_0. The absolute value of the temperature gradient $|\partial(\Delta T(r,z))/\partial r|$ versus r/w_0 is also plotted for explaining the origin of the divergence of the laser beam. We can see from Fig. 1 that the two curves coincide with each other. This confirms to us that the divergence of laser beam is contributed to the temperature gradient in the MF, which will redistribute the concentration.

As shown in Fig. 1, there is a maximum divergence angle $\theta_{\max}$ assigned to the beam ray at r_0. By solving $d\theta/dr=0$, we can get $r_0\approx 0.7926\ w_0$ and then

$$\theta_{\max} = \theta(r=r_0) \approx \frac{0.1083\ P}{\pi\kappa n_0 w_0}\left|\frac{dn}{dT}\right|(1-e^{-\alpha L}) = BP, \tag{6}$$

where B is a constant depending on the MF and the spot size of the incident laser.

From Fig. 1, we can also see that there are two sets of beam rays that have the same divergence angles. These two sets of rays will interfere constructively or destructively in the far field depending on the optical path-length difference between them, so the donutlike spherical aberration interference rings will be formed on the screen. The inset of Fig. 1 displays the propagation of the beam rays in the free space after passing through the sample. We only plot the propagation of the beam rays within $r<2w_0$, which contain 99.9877% power of the total laser beam. It is reasonable to assume that all the beam rays on the MF are confined to $r<2w_0$. It is clear from this inset that there are two sets of beam rays: $r<r_0$ (denoted by blue lines) and $r>r_0$ (denoted by red lines), which have the same divergence angles. They will interfere with each other on the screen. These simulation results explain the emergence of the spherical aberration interference rings.

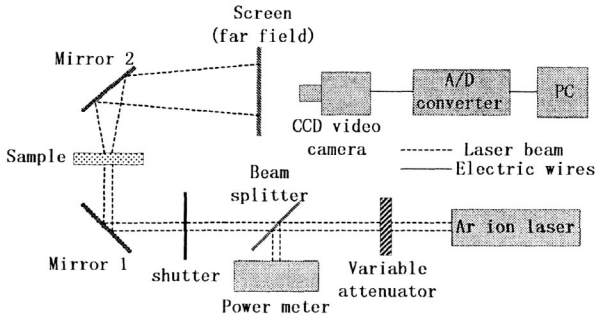

FIG. 2. The schematics of experimental setup for studying the thermo-optical effects in MF.

The MF is sealed in a sample cell made of two glass plates with a spacing of 50 μm. The sample is a thin cylinderlike and the area of its cross section is much larger than the spot size of the incident laser, thereby the part far from the optical-centered axis is unaffected by the laser beam.

Figure 2 shows the experimental setup for studying the thermo-optical effects in MF. A cw argon-ion laser with a wavelength of 514.5 nm is used. The variable attenuator is introduced in the light path to change the incident laser power on the sample. A splitter is used to reflect a small quantity of power to the power meter to monitor the incident power. The emergent rays are divergent and imagined on the screen. The interference patterns and the spot diameters on the screen are recorded by a charge-coupled device (CCD) video camera. An analog-to-digital converter is employed to transfer the signals from the CCD video camera to a personal computer. The shutter is placed between the beam splitter and mirror 1 to avoid the sample irradiating by the laser beam between the two experimental data. During this time, the irradiated region of the sample will return to its initial state. The length of the optical path between the Argon-ion laser and the sample is $L_1=390$ mm and the length between the sample and the screen is $L_2=600$ mm.

Figure 3 displays the typical steady-state patterns on the screen recorded by the CCD video camera at different incident powers, (a) 0.8, (b) 2.9, (c) 5.1, and (d) 10.1 mW. Figure 3(a) shows the facular spot on the screen at 0.8 mW. Only the divergence of the laser beam occurs at this power, while spherical aberration interference rings do not appear. The relationship between the number of interference rings N and the maximum phase change $\delta\phi_{\max}$ can be estimated by $\delta\phi_{\max}=2\pi N$.[11] Because of low laser power, the maximum phase change does not accumulate to 2π so that no interference ring is observed. In our experimental observations, the spherical aberration interference rings happen when the incident power is beyond 1 mW. From Figs. 3(b) and 3(c), we can see that the degree of divergence of the laser beam and the number of interference rings N will increase with the

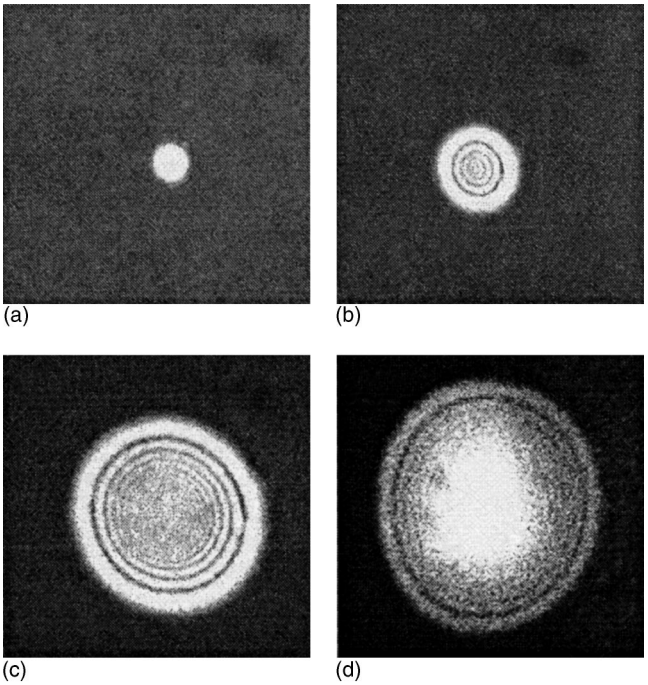

FIG. 3. Typical steady-state patterns at different incident powers: (a) 0.8, (b) 2.9, (c) 5.1, and (d) 10.1 mW.

incident power. A too high incident power will make the image of the interference rings fuzzy, as shown in Fig. 3(d).

The spot diameter from the laser window is $d_0 = 1.3$ mm and becomes $d = 2.0$ mm on the screen when the sample is removed. So, the spot diameter on the sample can be calculated to be $d_s = 1.5758$ mm using the values of L_1 and L_2. The intrinsic divergence angle of the laser beam is calculated to be $\theta_0 = 3.5354 \times 10^{-4}$ rad. By measuring the spot size d on the screen, we can get the divergence angle using $\theta = \theta_0 + \theta_{\max} = \arctan[(d - d_s)/1200]$. Figure 4 plots the divergence angles calculated according to this formula as a function of incident power. We can see that the divergence angle is linearly proportional to the input power up to 8 mW. To the too high power side, the curve deviates from the linear

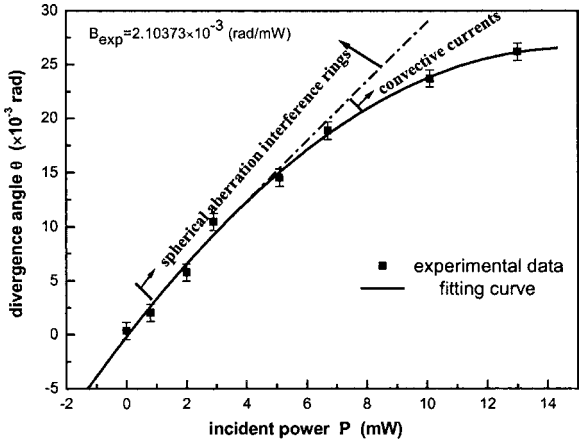

FIG. 4. Divergence angle vs incident power.

relationship. This is assigned to the occurrence of the convective currents in the MF when the temperature gradient exceeds a critical value.[22,23] This effect will blur the interference rings, as shown in Fig. 3(d).

The slope of the linear part in Fig. 4 is $B_{\exp} = 2.10373 \times 10^{-3}$ rad/mW when fitting the data to the function $\theta = \theta_0 + \theta_{\max} = \theta_0 + BP$. Substituting $\alpha = 120$ cm^{-1}, $L = 5 \times 10^{-3}$ cm, $\kappa = 7.56 \times 10^{-5}$ cal cm^{-1} s^{-1} K^{-1}, $n_0 = 1.5$, and $w_0 = d_s/2 = 0.07879$ cm into Eq. (6), we can get

$$B = 1.7408 \left| \left(\left. \frac{\partial n}{\partial T} \right|_c + \frac{\partial n}{\partial c} \frac{\partial c}{\partial T} \right) \right| \text{(rad/mW)}. \tag{7}$$

Chen *et al.* have found that the thermo-optical coefficient of MF is negative and less than 10^{-4} K^{-1} by experiment.[24] Comparing Eq. (7) with $B_{\exp}$ using $|[(\partial n/\partial T)|_c]| < 10^{-4}$ K^{-1}, it is obvious that the second term assigned to the concentration distribution dominates the expression, while the first term, which is induced by the thermal expansion, can be negligible compared with the second term. Finally, we would like to point out that Du and Luo got the analogous results by a numerical simulation.[11]

In summary, we have investigated the laser self-induced thermo-optical effects in the MF theoretically and experimentally. The linear relationship between the divergence angle of the laser beam and the incident power is obtained in the low power range. The convective currents will happen at a high incident power. This will damage the linear relationship and make the interference patterns fuzzy. The results presented in this paper may be useful for designing the MF-based optical devices.

This research was supported by the National Natural Science Foundation of China (Grant No. 60477016) and the Foundation for Development of Science and Technology of Shanghai (Grant No. 04DZ14001).

[1] R. E. Rosensweig, *Ferrohydrodynamics* (Cambridge University Press, Cambridge, 1985).
[2] W. E. L. Haas and J. E. Adams, Appl. Phys. Lett. **27**, 571 (1975).
[3] P. C. Scholten, IEEE Trans. Magn. **16**, 221 (1980).
[4] C.-Y. Hong, J. Magn. Magn. Mater. **201**, 178 (1999).
[5] H. E. Horng *et al.*, Appl. Phys. Lett. **79**, 350 (2001).
[6] S. Y. Yang *et al.*, Appl. Phys. Lett. **79**, 2372 (2001).
[7] A. F. Bakuzis *et al.*, Appl. Phys. Lett. **84**, 2355 (2004).
[8] H. E. Horng *et al.*,Appl. Phys. Lett. **82**, 2434 (2003).
[9] M. Xu and P. J. Ridler, J. Appl. Phys. **82**, 326 (1997).
[10] T. Du, S. Yuan, and W. Luo, Appl. Phys. Lett. **65**, 1844 (1994).
[11] T. Du and W. Luo, Appl. Phys. Lett. **72**, 272 (1997).
[12] W. Luo, T. Du, and J. Huang, J. Magn. Magn. Mater. **201**, 88 (1999).
[13] G. Liberts, Y. Mitrofanov, and A. Cebers, Proc. SPIE **5123**, 94 (2003).
[14] J. P. Gordon *et al.*, R. S. Moore, S. P. S. Porto, and J. R. Whinnery, J. Appl. Phys. **36**, 3 (1965).
[15] S. A. Akhmanov *et al.*, IEEE J. Quantum Electron. **QE-4**, 568 (1968).
[16] M. Giglio and A. Vendramini, Appl. Phys. Lett. **25**, 555 (1974).
[17] R. C. C. Leite *et al.*, and J. R. Whinnery, Appl. Phys. Lett. **5**, 141 (1964).
[18] D. Solimini, J. Appl. Phys. **37**, 3314 (1966).
[19] A. Marcano *et al.*, Appl. Phys. Lett. **78**, 3415 (2001).
[20] F. W. Dabby *et al.*, Appl. Phys. Lett. **16**, 362 (1970).
[21] Zs. Benkö *et al.*, Proc. SPIE **3407**, 285 (1998).
[22] J. R. Whinnery *et al.*, IEEE J. Quantum Electron. **QE-3**, 382 (1967).
[23] H. Inaba and H. Ito, IEEE J. Quantum Electron. **QE-4**, 45 (1968).
[24] Y. F. Chen *et al.*, Appl. Phys. Lett. **82**, 3481 (2003).